

THROMBOSIS AND HEMOSTASIS

Genome editing of factor X in zebrafish reveals unexpected tolerance of severe defects in the common pathway

Zhilian Hu,¹ Yang Liu,^{1*} Michael C. Huarng,¹ Marzia Menegatti,² Deepak Reyon,^{3,4**} Megan S. Rost,¹ Zachary G. Norris,¹ Catherine E. Richter,¹ Alexandra N. Stapleton,¹ Neil C. Chi,⁵ Flora Peyvandi,² J. Keith Joung,^{3,4} and Jordan A. Shavit¹

¹Department of Pediatrics and Communicable Diseases, University of Michigan, 1150 West Medical Dr., Ann Arbor, MI 48109-5646, USA

²Angelo Bianchi Bonomi Hemophilia and Thrombosis Centre, Fondazione IRCCS Ca' Granda Ospedale Maggiore Policlinico, Department of Pathophysiology and Transplantation, Università degli Studi di Milano, and Fondazione Luigi Villa, Milan, Italy

³Molecular Pathology Unit, Center for Computational and Integrative Biology, and Center for Cancer Research, Massachusetts General Hospital, 149 13th Street, 6th Floor, Charlestown, MA 02129, USA

⁴Department of Pathology, Harvard Medical School, Boston, MA, USA

⁵Department of Medicine, Division of Cardiology, University of California, San Diego, La Jolla, CA 92093, USA

Present address: *Molecular Innovations, Inc., Novi, MI. **Editas Medicine, Cambridge, MA.

Correspondence: Jordan Shavit, Department of Pediatrics, University of Michigan, Room 8301 Medical Science Research Building III, 1150 W. Medical Center Dr., Ann Arbor, MI 48109-5646; e-mail: jshavit@umich.edu
Phone: 734-647-4365
FAX: 734-764-4279

Running title: Loss of factor X in zebrafish

Word counts:

Abstract (words): 245

Text (words): 3949

Figures: 7

Tables: 0

References: 70

Supplementary Figures: 5

Supplementary Tables: 5

Key Points

- Deficiency of coagulation factor X in zebrafish results in a severe hemostatic defect that is surprisingly well tolerated until adulthood.
- *In vivo* analysis of human mutations in zebrafish identifies variants underlying symptomatic factor X deficiency.

ABSTRACT

Deficiency of factor X (F10) in humans is a rare bleeding disorder with a heterogeneous phenotype and limited therapeutic options. Targeted disruption of *F10* and other common pathway factors in mice results in embryonic/neonatal lethality with rapid resorption of homozygous mutants, hampering further studies. Several of these mutants also display yolk sac vascular defects, suggesting a role for thrombin signaling in vessel development. The zebrafish is a vertebrate model that demonstrates conservation of the mammalian hemostatic and vascular systems. We have leveraged these advantages for in depth study of the role of the coagulation cascade in developmental regulation of hemostasis and vasculogenesis. Here we show that ablation of zebrafish *f10* using genome editing TALENs results in a major embryonic hemostatic defect. However, widespread hemorrhage and subsequent lethality does not occur until later stages, with absence of any detectable defect in vascular development. We also use *f10*^{-/-} zebrafish to confirm five novel human *F10* variants as causative mutations in affected patients, providing a rapid and reliable *in vivo* model for testing the severity of *F10* variants. These findings as well as the prolonged survival of *f10*^{-/-} mutants will enable us to expand our understanding of the molecular mechanisms of hemostasis, including a platform for screening variants of uncertain significance in patients with F10 deficiency and other coagulation disorders. Further study as to how fish tolerate what is an early lethal mutation in mammals could facilitate improvement of diagnostics and therapeutics for affected patients with bleeding disorders.

INTRODUCTION

Coagulation factor X (F10) is a vitamin K-dependent plasma glycoprotein that is one of the pivotal factors in the coagulation cascade. F10 consists of eight domains, is synthesized in the liver as a single chain precursor, and circulates in human plasma.^{1,2} The conversion of F10 from zymogen to its active form (F10a) is triggered by the tenase complex and is important for both initiation and propagation of coagulation.³⁻⁵ Activated F10 participates in the formation of the prothrombinase complex, catalyzing the conversion of prothrombin to thrombin, a critical step for normal physiologic hemostasis.⁶

Deficiency of F10 leads to a rare inherited autosomal recessive coagulopathy, with the most severe bleeding arising early in life.^{2,7} It represents 10% of rare bleeding disorders and occurs in 1 per 500,000 to 1,000,000 of the general population.^{2,7-10} The clinical symptoms of homozygotes range from mild to severe hemorrhage, and currently more than 100 naturally occurring mutations in *F10* have been identified, among which 78% are missense.^{2,7} Most reported mutations have been found in the N-terminal light chain, particularly the γ -carboxyglutamic acid (Gla) domain, or the C-terminal heavy chain containing the catalytic domain.⁷ The vast majority of these mutations remain relatively uncharacterized. Current treatment includes the administration of plasma or prothrombin complex concentrates containing F10 and other vitamin K-dependent factors. Additional therapies for control of bleeding are still needed, as current options are limited.⁹

Previous studies using gene targeting in mice have facilitated understanding of F10 and common pathway function, but were impeded by embryonic and neonatal lethality in homozygous mutants.¹¹⁻¹⁴ These studies also suggested a role for thrombin signaling in embryonic vascular development, but this has been technically difficult to confirm.¹⁵ Thus we have turned to the zebrafish model (*Danio rerio*) with advantages that include high fecundity, external and transparent development, ease of manipulation and maintenance, accessibility of genetic techniques and imaging, as well as extensive conservation of the hemostatic and vascular systems as we and others have demonstrated.¹⁶⁻³⁰

Here we report targeted mutagenesis of zebrafish *f10* through genome editing with transcription activator-like effector nucleases (TALENs). We find that loss of F10 results in late onset lethality by four months of age secondary to intracranial and intra-abdominal hemorrhage, without any evidence for a vascular defect. Severe overt hemorrhage does not occur until approximately 1 month of age despite absence of hemostasis as early as 3 days post fertilization (dpf). We also use our model as an *in vivo* system to evaluate human *F10* variants of uncertain

significance (VUS) from 5 patients with symptomatic F10 deficiency whose causative mutations were not yet proven. Our studies demonstrate that loss of zebrafish F10 results in phenotypes similar to mice and humans, yet with surprising tolerance to what is a severe insult in mammals. This implies species-specific differences that, if understood, could suggest novel mechanisms for controlling hemorrhage in patients with and without bleeding disorders.

METHODS

Zebrafish strains and maintenance

f10 mutants were generated on a hybrid background of wild type strains AB and TL (ABxTL). Developmental stages were defined as follows: embryo (0 to 2 dpf), larva (3 to 29 dpf), juvenile (30 to 89 dpf), and adult.³¹ Pigmentation was inhibited with 0.2 mM phenylthiourea (Sigma-Aldrich).³² All animal experiments were in accordance with guidelines approved by the University of Michigan Animal Care & Use Committee.

Targeted mutagenesis of the *f10* locus using genome editing nucleases

The *f10* locus was identified in the zebrafish genomic sequence assembly¹⁶ and TALEN mediated genome editing used to induce mutations in exon 5. TALEN constructs were prepared using FLASH assembly,³³ and validated as described.^{22,34} TALEN mRNAs were synthesized and injected into the cytoplasm of 1-cell stage embryos. The resulting F0 population was raised to adulthood and crossed to wild type fish to confirm germline transmission to the F1 generation.

Genotyping of mutant offspring

Staged zebrafish were anesthetized in tricaine (0.16 mg/mL, Western Chemical) and fin-clipped for survival studies^{35,36} or humanely killed in high-dose tricaine (1.6 mg/mL) followed by genotyping of tail biopsies or whole fish. Genomic DNA was isolated using lysis buffer (10 mM Tris-Cl, pH 8.0; 2 mM EDTA, 2% Triton X-100, and 100 µg/mL Proteinase K) at 55°C overnight.²² Proteinase K was inactivated by heating for 5 minutes at 95°C. PCR was performed using gene specific primers (Table S1).

Laser-mediated endothelial injury in zebrafish larvae

Laser-mediated injury was performed on the endothelium of the posterior cardinal vein (PCV) of larvae as previously described.^{22,37,38} Three dpf larvae were anesthetized, embedded in agarose (0.8%), and PCV endothelium ablated with a laser at the 5th somite distal to the anal pore (MicroPoint Pulsed Laser System, Andor Technology). The time to complete occlusion was recorded by an observer blinded to genotype for up to 2 minutes. Following ablation, larvae were recovered from agarose and genotyped.

Chemical treatment of embryos

Embryos were incubated in 100 mM ϵ -aminocaproic acid (Sigma) or 10 µg/mL warfarin (Sigma) dissolved in system water or E3 medium (5 mM NaCl, 0.17 mM KCl, 0.33 mM CaCl₂,

0.33 mM MgSO₄), respectively, at 1 dpf. The former were evaluated at 3 dpf by laser-mediated endothelial injury, and the latter stained at 7 dpf using o-dianisidine for detection of hemoglobin.^{39,40}

Phylogenetic analysis

F10 protein sequences were retrieved from NCBI, EMBL, and ENSEMBL genome databases. Sequence alignments were performed using ClustalW2, and phylogenetic trees constructed by the neighbor-joining method.

Statistical analysis

Statistical analysis was performed using the Mann-Whitney *U* or two-tailed Student t-tests. Survival curves were generated using Prism (Graphpad Software) and evaluated by log-rank (Mantel-Cox) testing for significance.

RESULTS

Spatiotemporal expression profiles of *f10* in developing zebrafish

The predicted protein sequence of zebrafish F10 was compared with various species for phylogenetic analysis. The resulting tree indicated that the zebrafish F10 protein was more closely related to chicken than mouse or human (Figure 1A). We analyzed the expression of zebrafish *f10* mRNA during embryonic and early larval development by RT-PCR and WISH. *f10* expression was detected in embryos as early as the 1-cell stage and in larvae up to 120 hours post fertilization (hpf) (Figure 1B). Transcription of *f10* at the 1- and 4-cell stages indicates maternal contribution as zygotic expression does not begin until 2.75 hpf.³¹ At 4 hpf, both maternal and zygotic expression appeared to be present as *f10* was strongly transcribed compared to earlier and later stages (Figure 1B), suggesting crossover from maternal to zygotic *f10* transcription. From 24 hpf onwards, *f10* was found to be transcribed at relatively stable levels up to 120 hpf (Figure 1B). WISH and histological analysis of zebrafish larvae at 120 hpf revealed that *f10* expression is localized to the brain, jaw, and pharyngeal arches (Figure 1C-F, H-I), in addition to the otic vesicle, liver, and yolk syncytial layer (Figure 1D-E, G, J-L). Our data also showed that *f10* was transcribed much more strongly in the liver than other tissues (Figure 1D-L).

Targeted inactivation of the *f10* gene using genome editing nucleases results in spontaneous hemorrhage and lethality in juveniles and adults

To create a model of *f10* deficiency, we ablated the zebrafish *f10* gene using genome editing TALENs. We designed a TALEN pair targeting the 5th exon of *f10* (Figure 2A) and mRNAs encoding these nucleases were injected into ABxTL wild type 1-cell embryos. The resulting F0 generation was raised and outcrossed to ABxTL to produce the F1 generation. We identified a mutant line with germline transmission of a 17 base pair deletion in exon 5, resulting in a frameshift and downstream nonsense mutation (Figure 2B). Quantitative PCR analysis was not able to detect transcription of *f10* in 3 dpf homozygous mutant larvae in comparison to *f10*^{+/+} and *f10*^{+/-} siblings (p=0.0001, Figure 2C), presumably due to nonsense-mediated decay.⁴¹ WISH demonstrated no expression of *f10* mRNA in homozygous mutant larvae (Figure 2D). Transcription of other coagulation factors downstream of F10 was distinctly altered in a dose dependent fashion (Figure S1). This included increases in *f10* homozygous mutants of 1.8 and 2.3-fold for *fga* (fibrinogen alpha) and *at3* (antithrombin III) mRNAs, respectively (p<0.05, Figure S1), when compared to wild type siblings. Prothrombin (*f2*) transcription was slightly decreased, although the effect was not statistically significant (Figure S1). In order to ensure that modest changes in size did not cause these results, we measured 3 dpf larvae, but found no correlation with genotype (Figure S1D).

Loss of F10 in mice results in a bimodal phenotype of embryonic and neonatal lethality.¹⁴ In a group of closely monitored heterozygous incrosses, we found that there was no specific loss of zebrafish *f10*^{-/-} mutants during embryonic development and the larval period, through approximately 16 dpf (Figure 3A). There was a brief period of a 20% general population loss from ~10-16 dpf, which is typical for wild type zebrafish and was observed across all three genotypes (Figure 3B). After that point there was progressive loss of *f10*^{-/-} mutants (Figure 3B). By 50 dpf 75% of *f10*^{-/-} mutants had expired, and 100% by 4 months of age (Figure 3B). This phenotype has been consistent in our *f10* mutant breeding colony since then, although out of a total of 71 homozygous mutants identified thus far, one survived for 268 days. To determine whether coagulation was intact in mutants, we performed a thrombin activity assay on plasma at 1 month of age. The results indicate absence of activity specifically in homozygotes, suggestive of defective prothrombin activation (Figure 3C).

Given the embryonic hemorrhage exhibited in the mouse knockout, we carefully examined zebrafish at early stages of development. A low but non-significant frequency of intracranial hemorrhage was observed in *f10*^{-/-} larvae at 3 dpf (1.33%, n=225), while no bleeds were observed in their *f10*^{+/+} (n=221) and *f10*^{+/-} (n=465) siblings. In order to prospectively evaluate homozygous mutants, we genotyped *f10*^{+/-} intercross offspring at 3 dpf, followed by daily visual phenotypic assessments. At 27 dpf approximately one third of viable *f10*^{-/-} fish exhibited massive hemorrhage in the forebrain, midbrain, and hindbrain ventricles (Figure 4A), others displayed bleeding in the eye, muscle, or other tissues, and some appeared normal. Once gross hemorrhage became visible, the majority of *f10*^{-/-} mutants died within 5 days. The mutants lacking intracranial or grossly visible bleeds tended to survive longer and exhibit intracranial, intra-abdominal, or gill hemorrhage at later stages (e.g. 39 dpf, Figure 4A and data not shown). We performed histologic sections in *f10* mutants from 27 to 268 dpf (Table S3), confirming the suspected hemorrhage in brain, muscle, and abdomen (Figure 4B).

Deficiency of F10 does not appear to affect vascular development in zebrafish

Loss of function studies of the common pathway coagulation factors F2 and factor V (F5) in mice have shown embryonic lethality with vascular abnormalities and hemorrhage, while fibrinogen knockouts develop normally, suggesting a role for thrombin signaling in vessel development.¹⁵ The external growth of zebrafish has been instrumental in the study of angiogenesis and vasculogenesis, thus offering an alternative approach to assess whether F10 plays a role in vascular development.^{26,30} We evaluated the spatiotemporal expression patterns of vascular genes *ephb2a*,^{42,43} *cdh5*,⁴⁴ *flkl*,^{45,46} *flt4*,⁴⁷ and *ephb4*⁴² in offspring from *f10*^{+/-} incrosses

by WISH, followed by genotyping. Our results did not show any differences in the qualitative expression patterns between homozygous mutants and sibling controls at 24 hpf (data not shown) when axial and several intersegmental vessels are formed,^{48,49} or at 72 hpf (Figure S2) during the early stages of establishment of the vascular network.⁴⁸ We performed RNAseq on pools of wild type and homozygous mutant larvae at 72 hpf, but did not find any quantitative differences in these markers (Table S4). Next we crossed the *f10* mutants into a transgenic line in which the endothelium is labeled with mCherry (*Tg(flk1:mCherry/NTR)*). Embryos from an incross of *f10*^{+/-}; *Tg(flk1:mCherry/NTR)* fish were evaluated from 24 through 96 hpf. No aberrant sprouting or failure to sprout was observed at 24 hpf, and no signs of abnormal vasculature formation were observed. We measured the intersegmental vessel length from the posterior cardinal vein (PCV) to the dorsal longitudinal anastomotic vessel, and observed no significant differences in homozygous mutants (Figure S3). Genotyping was performed after phenotypic observation and confirmed the presence of all 3 expected genotypes.

Dysregulated apoptosis has been shown to cause loss of vascular integrity,²⁹ and F10 has been implicated in apoptosis through PAR-1 signaling.⁵⁰ To detect apoptotic cells, we stained larvae with acridine orange^{51,52} or probed with an antibody to caspase 3,⁵³ followed by blinded phenotypic observation and subsequent genotyping. We did not observe any differences in *f10*^{-/-} mutants versus their siblings (Figure S4), suggesting deficiency of F10 does not affect cellular apoptosis.

Loss of F10 results in early induced hemostatic defects in larval zebrafish

The low frequency of visible hemorrhage in larvae was surprising, especially considering the severe phenotypes observed in *F10* knockout mouse embryos and neonates. To address whether F10 plays a role in early zebrafish hemostasis, we evaluated the time to occlusion using an induced model of venous thrombosis in the PCV of 3 dpf larvae (Figure 5A). We found that occlusion was absent in *f10*^{-/-} larvae when compared to their *f10*^{+/+} and *f10*^{+/-} siblings, the vast majority of which formed occlusive thrombi ($p < 0.0001$, Figure 5B). In order to confirm that this was specific to loss of F10 rather than off-target mutations due to genome editing, we injected a *ubi* promoter regulated wild type *f10* cDNA expression construct into 1-cell stage offspring from *f10*^{+/-} incrosses, and evaluated the time to occlusion in larvae at 3 dpf. Our results showed that 72% of injected *f10*^{-/-} larvae displayed statistically significant rescue of the ability to form an occlusive thrombus ($p = 0.0001$ by the Mann-Whitney *U* test, Figure 5C).

Pro- and anticoagulant compounds have no effect on the *f10*^{-/-} larval hemostatic defect

Given the unexpected survival of homozygous mutant fish into adulthood, we hypothesized that there could be alternative pathways for residual thrombin generation and fibrin formation. We therefore evaluated the ability of the fibrinolysis inhibitor, ε-aminocaproic acid, to reverse the lack of induced venous occlusion in *f10*^{-/-} larvae. We have previously shown that ε-aminocaproic acid reverses the lack of occlusion observed in fibrinogen-deficient *at3* mutants²². We incubated *f10*^{+/-} incross offspring in ε-aminocaproic acid beginning at 24 hpf and evaluated the time to PCV occlusion at 3 dpf. Our data reveal that although treatment with ε-aminocaproic acid did increase the number of *f10*^{-/-} larvae with a normal occlusion time (12.8% vs. 6.7% in controls), this result was not statistically significant (Figure 6). There were also no differences in time to occlusion for treated and untreated *f10*^{+/+} and *f10*^{+/-} siblings (Figure 6). We have previously shown that warfarin inhibits laser-mediated occlusion in the PCV,²² although the incidence of overt bleeding is minimal. Given the low frequency of spontaneous hemorrhage observed in *f10*^{-/-} larvae, we speculated that maternally-derived F10 might play a role in early mutant embryos and larvae. We treated 1 dpf embryos with warfarin and observed them for evidence of hemorrhage by o-dianisidine staining at 7 dpf, followed by genotyping. Our data revealed no differences in o-dianisidine staining between *f10*^{-/-} mutants and *f10*^{+/-} or *f10*^{+/+} siblings (Figure S5).

Identification of causative variants in human F10 deficiency through *in vivo* evaluation in zebrafish *f10*^{-/-} mutants

As sequencing costs continue to decline, VUS are increasingly being identified. Although *in vitro* assays can often discern between functional and silent mutations, a wide variety of alternative techniques may be required depending on the nature of the mutation, as has been shown with *BRCA2*.⁵⁴ As a proof of concept, we tested two known *F10* mutations in the catalytic domain associated with F10 deficiency, G262D and C390F² (Figure 7A), sites that are conserved across multiple vertebrate species (Figure 7B). To assess their ability to rescue the lack of thrombotic occlusion in *f10*^{-/-} larvae, we engineered these variants into the orthologous positions in the zebrafish *f10* cDNA expression vector. The resulting mutant plasmids were injected into 1-cell stage zebrafish embryos from *f10*^{+/-} incrosses, followed by laser-mediated endothelial ablation of the PCV at 3 dpf. No significant rescue was demonstrated, indicating the requirement for function of these residues across species and conservation of the mutant phenotype.

We sequenced *F10* in five patients with F10 deficiency and identified novel mutations not previously associated with this disorder. These variants are located in various domains of human F10, including the Gla (R68C), activation peptide (G173W, ΔT176_Q186), and catalytic domains (I323M, Q416L) (Table S5, Figure 7A). The affected positions are conserved across mammalian,

avian, and aquatic species (except for the $\Delta T176_Q186$ deletion, Figure 7A) and were engineered into the zebrafish *f10* expression vector, followed by injection and laser-mediated endothelial injury as described above. Our data show that catalytic domain variants (I323M and Q416L) revealed a trend towards rescue (29% and 36%, respectively), although the results were not statistically significant (Figure 7C). The variants in the Gla domain and activation peptide failed to show any signs of statistically significant rescue of the hemostatic defect (Figure 7C).

DISCUSSION

Here we report targeted mutagenesis of zebrafish *f10* using genome editing TALENs. Based on observations in the mouse, we expected spontaneous fatal hemorrhage during the embryonic/larval period. Indeed, appropriate hemostatic responses are absent following endothelial injury at 3 dpf. A very low percentage of *f10*^{-/-} larvae at that stage exhibited hemorrhage, but it was at a background level consistent with our wild type colony. To our surprise, *f10*^{-/-} mutants are able to tolerate what should be a severe insult, do not exhibit significant overt bleeding symptoms until 3-4 weeks of age, and the majority survive for several months. The visible hemorrhage that eventually ensues predominantly manifests at intracranial and to a lesser extent intra-abdominal and intramuscular sites, similar to symptoms observed in humans with severe F10 deficiency.^{2,7} These phenotypes are the presumed cause of lethality, occurring by 4 months of age, with a steep drop at 1-2 months of age. This stark reduction correlates with the onset of visible hemorrhage as well as the transition to adulthood and sexual maturity. This time period includes an increase in aggressive behaviors, which could be responsible for the accelerated loss of homozygous mutants. Knockout mice demonstrate a bimodal phenotype and approximately one third of homozygous mutant embryos are lost between days 9.5-12.5 *in utero*, with the remainder succumbing to hemorrhage within 3 weeks postnatally.¹⁵ The lack of early onset hemorrhage in our *f10* homozygotes might have suggested that the coagulation cascade did not evolve to be active during embryonic/larval development. However, we and others have shown that this is not the case (Refs.^{21,22,37} and this report). One limitation to the use of zebrafish for modeling human developmental biology is the absence of a placenta. There is a large body of work demonstrating that the coagulation cascade regulates placental development through protease-activated receptors rather than fibrin formation,^{55,56} which could explain the embryonic lethality observed in F10 knockout mice.

This is the second example of unexpected long term survival of a coagulation factor knockout in fish when compared to its mammalian counterpart. We have previously shown that targeted disruption of zebrafish *at3* results in survival up to 6 months of age,²² despite the fact that

complete loss is embryonic lethal in mice¹⁴ and has never been described in humans.¹⁰ There are several potential explanations for this discrepancy. Our data demonstrate maternal contribution to early embryonic expression of *f10*, which might provide some protection during development, but is unlikely to account for the observed long term survival. Another possibility is blood pressure, as ventricular and aortic pressures range 0.1-0.5 mmHg in larvae and 0.1-2.5 mmHg in adults.^{57,58} In mice, embryonic ventricular pressures are up to 10-fold higher⁵⁹ than fish larvae and adults exhibit pressures similar to humans. Furthermore, mouse lethality is often in the neonatal period and could be secondary to birth trauma. Alternatively, we speculate that protective species-specific coagulation factors may exist in fish. Teleost fish underwent a whole genome duplication after divergence from mammals approximately 320-350 million years ago,⁶⁰ although the majority of coagulation factors have remained single copy.^{61,62} Neofunctionalization and subfunctionalization of related coagulation factors may have occurred, and elucidation of potential alternative hemostatic pathways could suggest novel therapeutic biologics or drug targets in humans.

Disruption of zebrafish *fga* has been reported, with 40-100% survival of homozygous mutants at 4-5 months of age,⁶³ concordant with mouse knockout data that show variable adult survival.⁶⁴ Taken together, the phenotypes of specific deletion of coagulation factors show similarities between mammals and fish, with loss of fibrinogen better tolerated than disruption of factors within and regulating the common pathway and thrombin generation (i.e. *at3* and *f10*). This is consistent with data that thrombin has a multitude of effects beyond conversion of fibrinogen to fibrin.^{65,66} Previous studies of coagulation factor cross regulation have primarily focused on protein-protein interactions. We have found that loss of F10 results in upregulation of *fga* and *at3* mRNA expression, although alterations in protein levels or activity have not been confirmed. This suggests the possibility of underlying mechanisms that sense either the level of coagulation cascade activity (thrombin activity or fibrin production) or individual factor levels. It is conceivable that such interactions are what contribute to the greater severity seen in the loss of common pathway factors versus fibrinogen.

The phenotypes observed in mouse knockouts of common pathway factors has led to the hypothesis that thrombin signaling is required for vascular development during embryogenesis.^{11-13,15} *F10* knockouts did not exhibit a clear vascular defect, although there was hemorrhage and rapid embryo resorption that might have prevented visualization of vessel anomalies.^{14,15} It has been previously shown that pathways regulating vascular development are highly conserved across vertebrate species.^{26,30} Multiple vascular mutants have been described in zebrafish with intracranial hemorrhage as a primary phenotype secondary to various mechanisms, including defects in vascular development, patterning, integrity, and remodeling.²⁷⁻²⁹ Our analysis did not

reveal any such vascular phenotypes, suggesting that the consequences of F10 loss are solely defects in hemostasis. This implies that thrombin generation is not a key player in zebrafish vasculogenesis or operates through non-F10 dependent pathways. Alternatively, paralogous coagulation factors may have neofunctionalized and assumed new roles in zebrafish vasculogenesis.

Rapid improvements in sequencing technologies continue to spawn new and broader applications to basic, translational, and clinical research.⁶⁷ One of the major remaining challenges is the interpretation of VUS. For a number of coagulation factor substitutions, *in vitro* assays miscall functional versus silent mutations (e.g. von Willebrand factor^{68,69}). As has been shown for *BRCA2*,⁵⁴ the availability of alternative methods can aid in clarifying such variants. We have previously used transient transgenesis in mutant zebrafish larvae as an *in vivo* assay for examination of established human hemostatic variants.²² In this study, we take this a step further and evaluate previously unconfirmed candidate mutations in multiple domains from symptomatic patients with F10 deficiency. The patient phenotypes range from minor to major bleeding, with factor activities <1-5%. Five novel and two established substitutions or deletions are unable to rescue the *f10*^{-/-} hemostatic defect, thus confirming their pathogenicity. This platform will add to our armamentarium for coagulation factor analysis and has the advantage of not being susceptible to *in vitro* testing artifacts. However, it is important to note that despite the high degree of conservation across vertebrates, there is the possibility that species specific protein-protein interactions have developed that will limit this approach.

In conclusion, our findings that deficiency of F10 leads to loss of coagulation with massive hemorrhage yet paradoxical embryonic/larval survival provide a powerful alternative to studies in mammals. Overall our data align with the results of gene targeting in mice and observations in patients. However, the extended survival and external nature of zebrafish embryonic/larval development has already allowed further mechanistic investigation, including data suggesting that thrombin signaling does not regulate vascular development. This model could lead to the development of novel therapeutics through genetic and small molecule screening⁷⁰ and is a powerful system for the *in vivo* functional evaluation of human VUS.

ACKNOWLEDGEMENTS

The authors thank Dr. Weibin Zhou for technical support, and the University of Michigan Sequencing and Microscopy & Image Analysis cores, particularly Ms. Shelley Almburg for imaging support. We thank Colin Kretz and members of the Shavit laboratory for critical review of the manuscript.

This work was supported by the National Institutes of Health R01-HL124232, Hemophilia of Georgia Clinical Scientist Development Grant, National Hemophilia Foundation/Novo Nordisk Career Development Award, Bayer Hemophilia Awards Program (J.A.S.), National Institutes of Health T32-HL007622 (M.S.R.), National Institutes of Health (N.C.C.), and National Institutes of Health R01-GM088040 (J.K.J.). J.K.J. is the Jim and Ann Orr Massachusetts General Hospital Research Scholar. J.A.S. is the Diane and Larry Johnson Family Scholar of Pediatrics and Communicable Diseases.

AUTHORSHIP CONTRIBUTIONS

Z.H. designed and performed research, analyzed data, and wrote the manuscript; M.C.H. designed and performed research and analyzed data; Y.L., Z.G.N., D.R., and J.K.J. designed and performed research; N.C.C. provided reagents; M.M. and F.P. designed research; A.N.S., M.S.R., and C.E.R. performed research and analyzed data; and J.A.S. designed and supervised research, analyzed data, and wrote the manuscript.

CONFLICT OF INTEREST DISCLOSURES

J.A.S. has been a consultant for Bayer, Shire, CSL Behring, Grifols, and Octapharma. F.P. has received honoraria for participating as a speaker at satellite symposia and educational meetings organized by Bayer, Biotest, CSL Behring, Grifols, Novo Nordisk, and Sobi. She is recipient of research grant funding from Alexion, Biotest, Kedrion Biopharma, and Novo Nordisk paid to Fondazione Luigi Villa, and she has received consulting fees from Kedrion Biopharma, LFB and Octapharma. She is member of the Ablynx scientific advisory board. J.K.J. has financial interests in Beacon Genomics, Beam Therapeutics, Editas Medicine, Poseida Therapeutics, and Transposagen Biopharmaceuticals. J.K.J.'s interests were reviewed and are managed by Massachusetts General Hospital and Partners HealthCare in accordance with their conflict of interest policies. The remaining authors declare no competing financial interests.

REFERENCES

1. Furie B, Furie BC. The molecular basis of blood coagulation. *Cell*. 1988;53(4):505-518.
2. Menegatti M, Peyvandi F. Factor X deficiency. *Semin Thromb Hemost*. 2009;35(4):407-415.
3. Di Scipio RG, Hermodson MA, Yates SG, Davie EW. A comparison of human prothrombin, factor IX (Christmas factor), factor X (Stuart factor), and protein S. *Biochemistry*. 1977;16(4):698-706.
4. van Dieijen G, Tans G, Rosing J, Hemker HC. The role of phospholipid and factor VIIIa in the activation of bovine factor X. *J Biol Chem*. 1981;256(7):3433-3442.
5. Rao LV, Rapaport SI. Activation of factor VII bound to tissue factor: a key early step in the tissue factor pathway of blood coagulation. *Proc Natl Acad Sci U S A*. 1988;85(18):6687-6691.
6. Davie EW, Fujikawa K, Kisiel W. The coagulation cascade: initiation, maintenance, and regulation. *Biochemistry*. 1991;30(43):10363-10370.
7. Herrmann FH, Auerswald G, Ruiz-Saez A, et al. Factor X deficiency: clinical manifestation of 102 subjects from Europe and Latin America with mutations in the factor 10 gene. *Haemophilia*. 2006;12(5):479-489.
8. Peyvandi F, Menegatti M, Santagostino E, et al. Gene mutations and three-dimensional structural analysis in 13 families with severe factor X deficiency. *Br J Haematol*. 2002;117(3):685-692.
9. Brown DL, Kouides PA. Diagnosis and treatment of inherited factor X deficiency. *Haemophilia*. 2008;14(6):1176-1182.
10. Shavit JA, Ginsburg D. Hemophilias and Other Disorders of Hemostasis. In: Rimo DL, Pyeritz RE, Korf BR, eds. *Emery and Rimo's Principles and Practice of Medical Genetics*: Elsevier Science; 2013:1-33.
11. Cui J, O'Shea KS, Purkayastha A, Saunders TL, Ginsburg D. Fatal haemorrhage and incomplete block to embryogenesis in mice lacking coagulation factor V. *Nature*. 1996;384(6604):66-68.
12. Sun WY, Witte DP, Degen JL, et al. Prothrombin deficiency results in embryonic and neonatal lethality in mice. *Proc Natl Acad Sci U S A*. 1998;95(13):7597-7602.
13. Xue J, Wu Q, Westfield LA, et al. Incomplete embryonic lethality and fatal neonatal hemorrhage caused by prothrombin deficiency in mice. *Proc Natl Acad Sci U S A*. 1998;95(13):7603-7607.
14. Dewerchin M, Liang Z, Moons L, et al. Blood coagulation factor X deficiency causes partial embryonic lethality and fatal neonatal bleeding in mice. *Thromb Haemost*. 2000;83(2):185-190.
15. Rosen ED. Gene targeting in hemostasis. Factor X. *Front Biosci*. 2002;7:d1915-1925.
16. Howe K, Clark MD, Torroja CF, et al. The zebrafish reference genome sequence and its relationship to the human genome. *Nature*. 2013;496(7446):498-503.
17. Sheehan J, Templer M, Gregory M, et al. Demonstration of the extrinsic coagulation pathway in teleostei: identification of zebrafish coagulation factor VII. *Proc Natl Acad Sci U S A*. 2001;98(15):8768-8773.
18. Jagadeeswaran P, Sheehan JP. Analysis of blood coagulation in the zebrafish. *Blood Cells Mol Dis*. 1999;25(3-4):239-249.
19. Jagadeeswaran P, Gregory M, Day K, Cykowski M, Thattaliyath B. Zebrafish: a genetic model for hemostasis and thrombosis. *J Thromb Haemost*. 2005;3(1):46-53.
20. Ghosh A, Vo A, Twiss BK, et al. Characterization of zebrafish von Willebrand factor reveals conservation of domain structure, multimerization, and intracellular storage. *Adv Hematol*. 2012;2012:214209.
21. Vo AH, Swaroop A, Liu Y, Norris ZG, Shavit JA. Loss of fibrinogen in zebrafish results in symptoms consistent with human hypofibrinogenemia. *PLoS One*. 2013;8(9):e74682.

22. Liu Y, Kretz CA, Maeder ML, et al. Targeted mutagenesis of zebrafish antithrombin III triggers disseminated intravascular coagulation and thrombosis, revealing insight into function. *Blood*. 2014;124(1):142-150.
23. Weyand AC, Shavit JA. Zebrafish as a model system for the study of hemostasis and thrombosis. *Curr Opin Hematol*. 2014;21(5):418-422.
24. Huarng MC, Shavit JA. Simple and rapid quantification of thrombocytes in zebrafish larvae. *Zebrafish*. 2015;12(3):238-242.
25. Kretz CA, Weyand AC, Shavit JA. Modeling Disorders of Blood Coagulation in the Zebrafish. *Curr Pathobiol Rep*. 2015;3(2):155-161.
26. Lawson ND, Weinstein BM. Arteries and veins: making a difference with zebrafish. *Nat Rev Genet*. 2002;3(9):674-682.
27. Buchner DA, Su F, Yamaoka JS, et al. pak2a mutations cause cerebral hemorrhage in redhead zebrafish. *Proc Natl Acad Sci U S A*. 2007;104(35):13996-14001.
28. Jin SW, Herzog W, Santoro MM, et al. A transgene-assisted genetic screen identifies essential regulators of vascular development in vertebrate embryos. *Dev Biol*. 2007;307(1):29-42.
29. Santoro MM, Samuel T, Mitchell T, Reed JC, Stainier DY. Birc2 (clap1) regulates endothelial cell integrity and blood vessel homeostasis. *Nat Genet*. 2007;39(11):1397-1402.
30. Gore AV, Monzo K, Cha YR, Pan W, Weinstein BM. Vascular development in the zebrafish. *Cold Spring Harb Perspect Med*. 2012;2(5):a006684.
31. Kimmel CB, Ballard WW, Kimmel SR, Ullmann B, Schilling TF. Stages of embryonic development of the zebrafish. *Dev Dyn*. 1995;203(3):253-310.
32. Westerfield M. The Zebrafish Book. A Guide for the Laboratory Use of Zebrafish (*Danio rerio*) (ed 4th). Eugene, OR: University of Oregon Press; 2000.
33. Reyon D, Tsai SQ, Khayter C, Foden JA, Sander JD, Joung JK. FLASH assembly of TALENs for high-throughput genome editing. *Nat Biotechnol*. 2012.
34. Foley JE, Maeder ML, Pearlberg J, Joung JK, Peterson RT, Yeh JR. Targeted mutagenesis in zebrafish using customized zinc-finger nucleases. *Nat Protoc*. 2009;4(12):1855-1867.
35. Hu Z, Holzschuh J, Driever W. Loss of DDB1 Leads to Transcriptional p53 Pathway Activation in Proliferating Cells, Cell Cycle Deregulation, and Apoptosis in Zebrafish Embryos. *PLoS One*. 2015;10(7):e0134299.
36. Wilkinson RN, Elworthy S, Ingham PW, van Eeden FJ. A method for high-throughput PCR-based genotyping of larval zebrafish tail biopsies. *Biotechniques*. 2013;55(6):314-316.
37. Jagadeeswaran P, Carrillo M, Radhakrishnan UP, Rajpurohit SK, Kim S. Laser-induced thrombosis in zebrafish. *Methods Cell Biol*. 2011;101:197-203.
38. Rost MS, Grzegorski SJ, Shavit JA. Quantitative methods for studying hemostasis in zebrafish larvae. *Methods Cell Biol*. 2016;134:377-389.
39. Iuchi I, Yamamoto M. Erythropoiesis in the developing rainbow trout, *Salmo gairdneri* irideus: histochemical and immunochemical detection of erythropoietic organs. *J Exp Zool*. 1983;226(3):409-417.
40. Paffett-Lugassy NN, Zon LI. Analysis of hematopoietic development in the zebrafish. *Methods Mol Med*. 2005;105:171-198.
41. Kervestin S, Jacobson A. NMD: a multifaceted response to premature translational termination. *Nat Rev Mol Cell Biol*. 2012;13(11):700-712.
42. Lawson ND, Scheer N, Pham VN, et al. Notch signaling is required for arterial-venous differentiation during embryonic vascular development. *Development*. 2001;128(19):3675-3683.
43. Zhong TP, Rosenberg M, Mohideen MA, Weinstein B, Fishman MC. gridlock, an HLH gene required for assembly of the aorta in zebrafish. *Science*. 2000;287(5459):1820-1824.
44. Sumanas S, Joriniak T, Lin S. Identification of novel vascular endothelial-specific genes by the microarray analysis of the zebrafish cloche mutants. *Blood*. 2005;106(2):534-541.

45. Bussmann J, Lawson N, Zon L, Schulte-Merker S, Zebrafish Nomenclature C. Zebrafish VEGF receptors: a guideline to nomenclature. *PLoS Genet.* 2008;4(5):e1000064.
46. Sumoy L, Keasey JB, Dittman TD, Kimelman D. A role for notochord in axial vascular development revealed by analysis of phenotype and the expression of VEGF-2 in zebrafish *flh* and *ntl* mutant embryos. *Mech Dev.* 1997;63(1):15-27.
47. Thompson MA, Ransom DG, Pratt SJ, et al. The *cloche* and *spadetail* genes differentially affect hematopoiesis and vasculogenesis. *Dev Biol.* 1998;197(2):248-269.
48. Isogai S, Horiguchi M, Weinstein BM. The vascular anatomy of the developing zebrafish: an atlas of embryonic and early larval development. *Dev Biol.* 2001;230(2):278-301.
49. Isogai S, Lawson ND, Torrealday S, Horiguchi M, Weinstein BM. Angiogenic network formation in the developing vertebrate trunk. *Development.* 2003;130(21):5281-5290.
50. Borensztajn KS, Bijlsma MF, Groot AP, et al. Coagulation factor Xa drives tumor cells into apoptosis through BH3-only protein Bim up-regulation. *Exp Cell Res.* 2007;313(12):2622-2633.
51. Furutani-Seiki M, Jiang YJ, Brand M, et al. Neural degeneration mutants in the zebrafish, *Danio rerio*. *Development.* 1996;123:229-239.
52. Negroni JF, Lockshin RA. Activation of apoptosis and caspase-3 in zebrafish early gastrulae. *Dev Dyn.* 2004;231(1):161-170.
53. Palencia-Desai S, Rost MS, Schumacher JA, et al. Myocardium and BMP signaling are required for endocardial differentiation. *Development.* 2015;142(13):2304-2315.
54. Guidugli L, Carreira A, Caputo SM, et al. Functional assays for analysis of variants of uncertain significance in BRCA2. *Hum Mutat.* 2014;35(2):151-164.
55. Sood R, Kalloway S, Mast AE, Hillard CJ, Weiler H. Fetomaternal cross talk in the placental vascular bed: control of coagulation by trophoblast cells. *Blood.* 2006;107(8):3173-3180.
56. Aasrum M, Prydz H. Gene targeting of tissue factor, factor X, and factor VII in mice: their involvement in embryonic development. *Biochemistry (Mosc).* 2002;67(1):25-32.
57. Hu N, Sedmera D, Yost HJ, Clark EB. Structure and function of the developing zebrafish heart. *Anat Rec.* 2000;260(2):148-157.
58. Hu N, Yost HJ, Clark EB. Cardiac morphology and blood pressure in the adult zebrafish. *Anat Rec.* 2001;264(1):1-12.
59. Ishiwata T, Nakazawa M, Pu WT, Tevosian SG, Izumo S. Developmental changes in ventricular diastolic function correlate with changes in ventricular myoarchitecture in normal mouse embryos. *Circ Res.* 2003;93(9):857-865.
60. Glasauer SM, Neuhauss SC. Whole-genome duplication in teleost fishes and its evolutionary consequences. *Mol Genet Genomics.* 2014;289(6):1045-1060.
61. Hanumanthaiah R, Day K, Jagadeeswaran P. Comprehensive analysis of blood coagulation pathways in teleostei: evolution of coagulation factor genes and identification of zebrafish factor VIIi. *Blood Cells Mol Dis.* 2002;29(1):57-68.
62. Davidson CJ, Tuddenham EG, McVey JH. 450 million years of hemostasis. *J Thromb Haemost.* 2003;1(7):1487-1494.
63. Fish RJ, Di Sanza C, Neerman-Arbez M. Targeted mutation of zebrafish *fga* models human congenital afibrinogenemia. *Blood.* 2014;123(14):2278-2281.
64. Suh TT, Holmback K, Jensen NJ, et al. Resolution of spontaneous bleeding events but failure of pregnancy in fibrinogen-deficient mice. *Genes Dev.* 1995;9(16):2020-2033.
65. Minami T, Sugiyama A, Wu SQ, Abid R, Kodama T, Aird WC. Thrombin and phenotypic modulation of the endothelium. *Arterioscler Thromb Vasc Biol.* 2004;24(1):41-53.
66. Coughlin SR. Protease-activated receptors in hemostasis, thrombosis and vascular biology. *J Thromb Haemost.* 2005;3(8):1800-1814.
67. van Dijk EL, Auger H, Jaszczyzyn Y, Thermes C. Ten years of next-generation sequencing technology. *Trends Genet.* 2014;30(9):418-426.
68. Flood VH, Friedman KD, Gill JC, et al. Limitations of the ristocetin cofactor assay in measurement of von Willebrand factor function. *J Thromb Haemost.* 2009;7(11):1832-1839.

69. Flood VH, Lederman CA, Wren JS, et al. Absent collagen binding in a VWF A3 domain mutant: utility of the VWF:CB in diagnosis of VWD. *J Thromb Haemost.* 2010;8(6):1431-1433.
70. Santoriello C, Zon LI. Hooked! Modeling human disease in zebrafish. *J Clin Invest.* 2012;122(7):2337-2343.

FIGURE LEGENDS

Figure 1. Spatiotemporal expression of *f10* in the developing zebrafish. (A) Phylogenetic tree of F10 from zebrafish (*Danio*), mouse (*Mus*), chicken (*Gallus*), and human (*Homo*). (B) RT-PCR from whole embryos demonstrates that zebrafish *f10* mRNA is expressed during early embryonic development beginning at the 1-cell stage. Expression is relatively stable from 24 through 120 hpf. The expression of elongation factor 1 alpha (*elfa*) was used as an internal control. (C-L) WISH analysis of 120 hpf larvae shows that *f10* expression is strong in the liver (D) but relatively weak in the yolk syncytial layer and brain (D-F), optic vesicles (E and G), and arches (H-I) using an antisense probe (*f10-as*). (C) A sense control did not show any expression (*f10-s*). (J-L) Plastic sections (5 μ m) of stained larvae in transverse (J), sagittal (K), and coronal (L) planes are shown. b, brain; ch, ceratohyal (2nd visceral pharyngeal arch (VA)); li, liver; mc, mandibular cartilage (1st VA); ov, optic vesicles; sb, swim bladder; y, yolk; ysl, yolk syncytial layer. Anterior is towards the left in C-H, and towards the top in I. Scale bars (D for C-D, I for E-I): 100 μ m.

Figure 2. Genome editing of factor *f10* using TALENs results in a frameshift and null allele.

(A) Schematic diagram of TALENs used for targeted mutagenesis of *f10*. C-term, C-terminal domain; DBD, DNA-binding domain; N-term, N-terminal domain; FokI, FokI nuclease; NLS, nuclear localization signal. (B) Targeting of *f10* exon 5 using a TALEN resulted in frameshift mutations. Shown here is the 17 base pair deletion mutant used for subsequent studies. (C) Expression of *f10* mRNA is reduced in heterozygous and undetectable in homozygous mutants, as evaluated by RT-PCR (each genotype was evaluated in triplicate). (D) Whole-mount *in situ* hybridization with an antisense probe demonstrates absence of expression in *f10*^{-/-} mutants. Anterior is towards the left, and dorsal towards the top. Scale bar: 100 μ m.

Figure 3. Complete loss of F10 results in progressive adult lethality. (A) Genotype distributions of offspring from separate *f10*^{+/-} incrosses evaluated at various stages demonstrate

loss of homozygous mutants after 25 dpf. (B) Survival curves of closely monitored clutches of zebrafish offspring from *f10*^{+/-} incrosses demonstrate progressive loss of 75% of homozygotes by 50 dpf, and 100% by 115 dpf. There was no significant loss of heterozygotes ($p>0.05$ by log-rank testing). Larvae were genotyped at 3 dpf and selected individuals were observed daily. There was around 20% background loss of individual fish across all genotypes up to 20 dpf which is typical during wild type fish development. (C) Citrated plasmas from one month old fish were recalcified and incubated with human fibrinogen for 90 minutes and absorbance (405 nm) measured every 2 minutes. Data shown are the average of two experiments ($n=5$ total pairs of fish for each genotype). The average time to half maximal absorbance and maximum absorbance were calculated for each genotype and data analyzed using the Student *t* test. Bovine thrombin was used as a positive control.

Figure 4. Loss of F10 results in late onset hemorrhage at multiple sites. (A) Grossly visible hemorrhage occurred in *f10*^{-/-} mutant fish as early as 27 dpf, but not in wild type or heterozygous siblings. Massive hemorrhage was observed in the brain, muscle, gill filaments, and abdomen as shown in viable *f10*^{-/-} mutants. ad, abdomen; gf, gill filaments; fb, forebrain; mb, midbrain; hb, hindbrain. (B) Histologic sections of *f10*^{-/-} mutants confirmed substantial intracranial, abdominal, and intramuscular hemorrhage at 27 dpf. Arrows indicate sites of hemorrhage. Locations of magnified insets are indicated by the smaller boxes in the same panel. Anterior is towards the left, and dorsal towards the top. Scale bar: 100 μ m.

Figure 5. Absence of hemostasis in *f10* mutant larvae. (A) Schematic diagram of laser-induced endothelial injury of the posterior cardinal vein (PCV) at the 5th somite (s5) caudal to the anal pore in larvae at 3 dpf. Hemostasis was evaluated by documenting the time to occlusion up to 120 seconds (sec) after laser-induced endothelial injury. (B) The time to occlusion was significantly prolonged in *f10*^{-/-} larvae in comparison with *f10*^{+/+} and *f10*^{+/-} siblings ($p<0.0001$ by the Mann-

Whitney *U* test). (C) Injection of wild type zebrafish *f10* cDNA under control of the *ubiquitin* promoter into 1-cell stage embryos resulted in significant rescue of the hemostatic defect in 72% of *f10*^{-/-} larvae at 3 dpf when compared to uninjected mutants (*p*<0.05). Horizontal bars represent the median time to occlusion. ns, not significant.

Figure 6. Treatment with ϵ -aminocaproic acid does not reverse the hemostatic defect in *f10* mutants. Offspring from *f10*^{+/-} incrosses were treated with ϵ -aminocaproic acid at 24 hpf and tested for the ability to form a clot in the PCV in response to laser-mediated endothelial injury at 3 dpf, followed by genotyping. There was a slight increase in the percentage of occlusion in treated *f10*^{-/-} larvae (12.8% vs. 6.7% in controls). However, this was not statistically significant and likely represents background thrombus formation occasionally observed in homozygous mutants. Horizontal bars represent the median time to occlusion. ns, not significant.

Figure 7. *In vivo* functional evaluation identifies causative variants for human F10 deficiency. (A) Schematic diagram of the human F10 domain structure and position of known and suspected F10 variants associated with bleeding. PP, propeptide; Gla, Gla domain; EGF-1/2, epidermal growth factor-like domains; AP, activation peptide. (B) Multiple sequence alignment of peptides containing human F10 variants shows conservation across vertebrate species. Protein sequences are from human (NP_000495.1), mouse (NP_001229297.1), chicken (NP_990353.1), and zebrafish (NP_958870.2). The altered residues are marked by arrows. *Danio*, zebrafish; *Gallus*, chicken; *Homo*, human; *Mus*, mouse. (C) Human *F10* variants were engineered into the orthologous positions of the zebrafish *f10* cDNA and placed under the control of the *ubi* promoter. The expression vectors were injected into the cytoplasm of 1-cell stage offspring from *f10*^{+/-} incrosses. The endothelium of the PCV was injured by laser ablation at 3 dpf and the time to complete occlusion recorded, followed by genotyping. Numbering represents the human amino acid positions. The first two variants tested were G262D and C390F, both known to cause

clinically significant human F10 deficiency. The subsequent variants, R68C, G173W, Δ T176_Q186, I323M, Q416L, were identified in patients with F10 deficiency and clinically significant bleeding, but not yet proven to be causative. Although I323M and Q416L showed a trend towards occlusion, none of the variants examined were able to significantly rescue the hemostatic defect of mutants ($p < 0.001$ by Mann-Whitney U test). Horizontal bars represent the median time to occlusion. $n \geq 18$ for each variant tested.

FIGURES

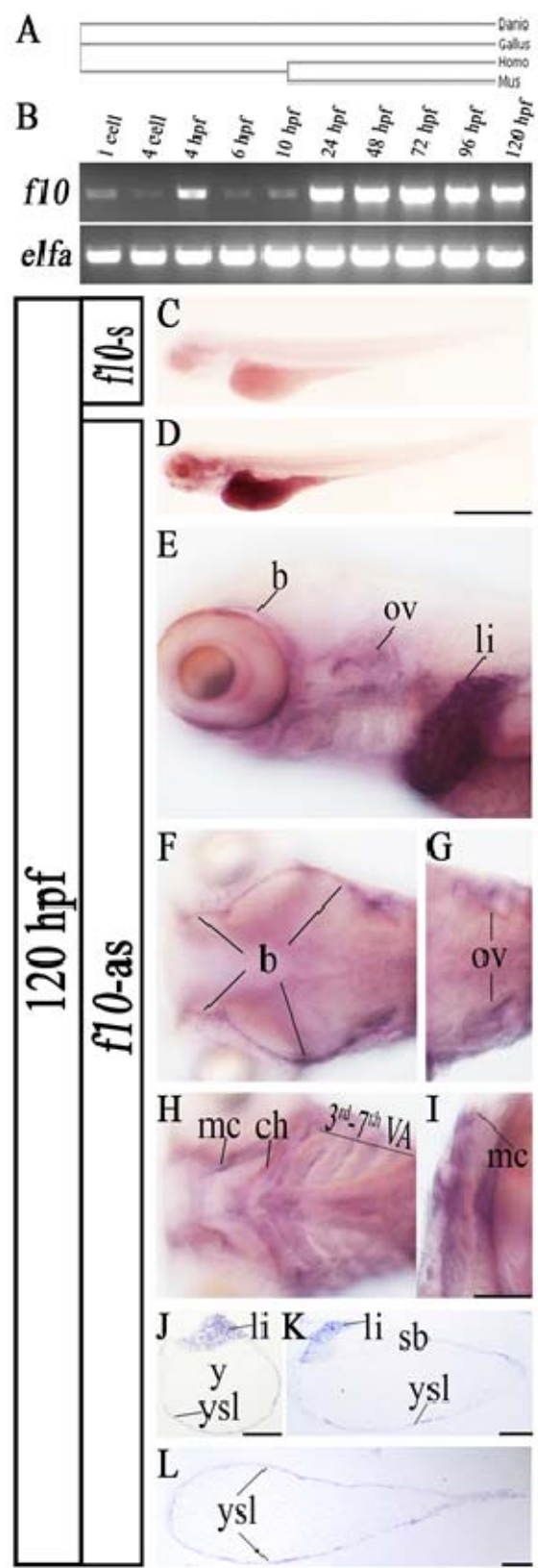


Figure 1

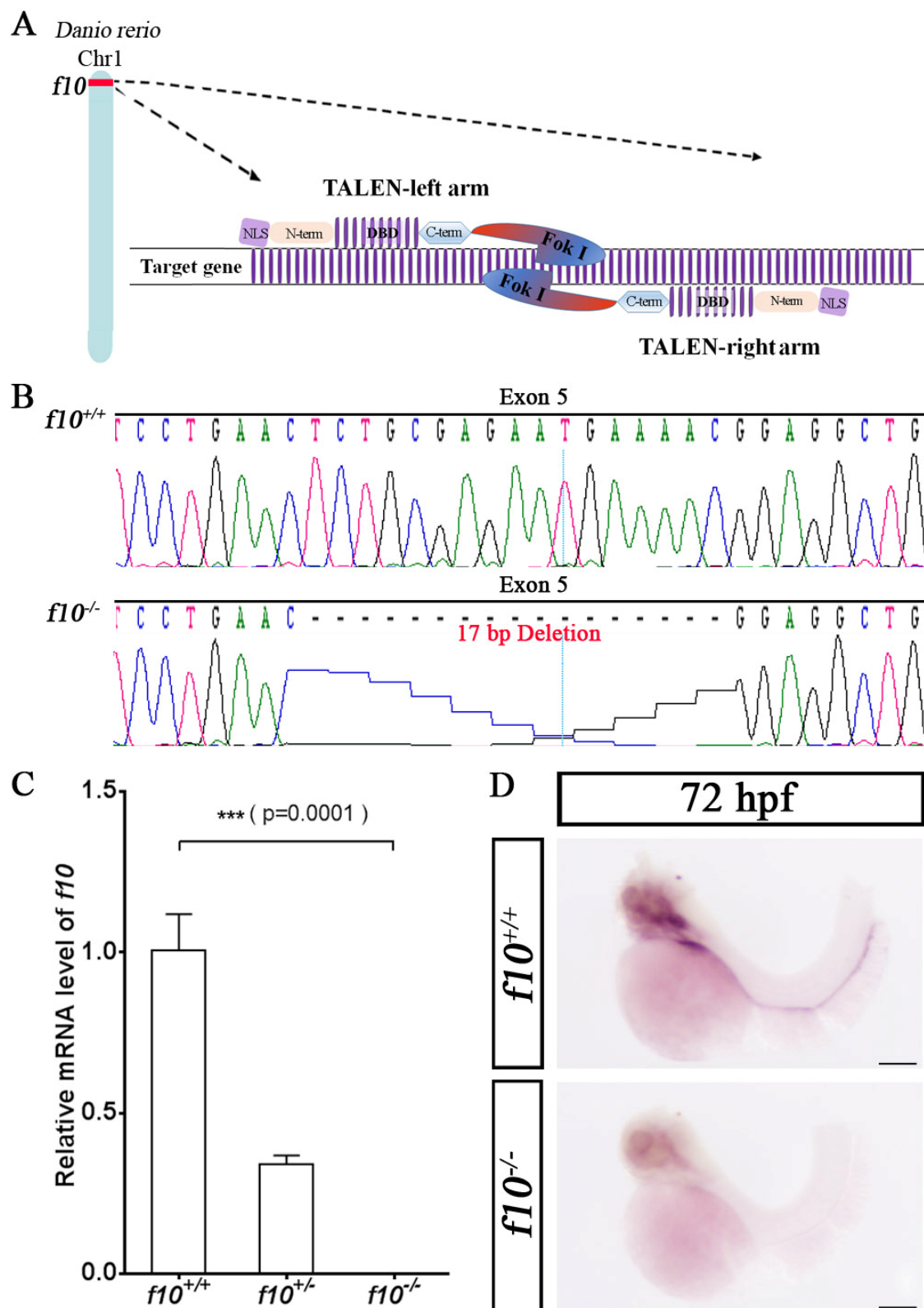


Figure 2

A Genotype distribution among the offspring of $f10^{+/-}$ intercross

Stage	$f10^{+/+}$	$f10^{+/-}$	$f10^{-/-}$	Total
3 dpf	162 (23%)	371 (53%)	173 (25%)	706 (100%)
15 dpf	10 (28%)	17 (47%)	9 (25%)	36 (100%)
25 dpf	19 (26%)	34 (47%)	19 (26%)	72 (100%)
90 dpf	13 (22%)	39 (67%)	6 (10%)	58 (100%)
Mendelian traits	25%	50%	25%	100%

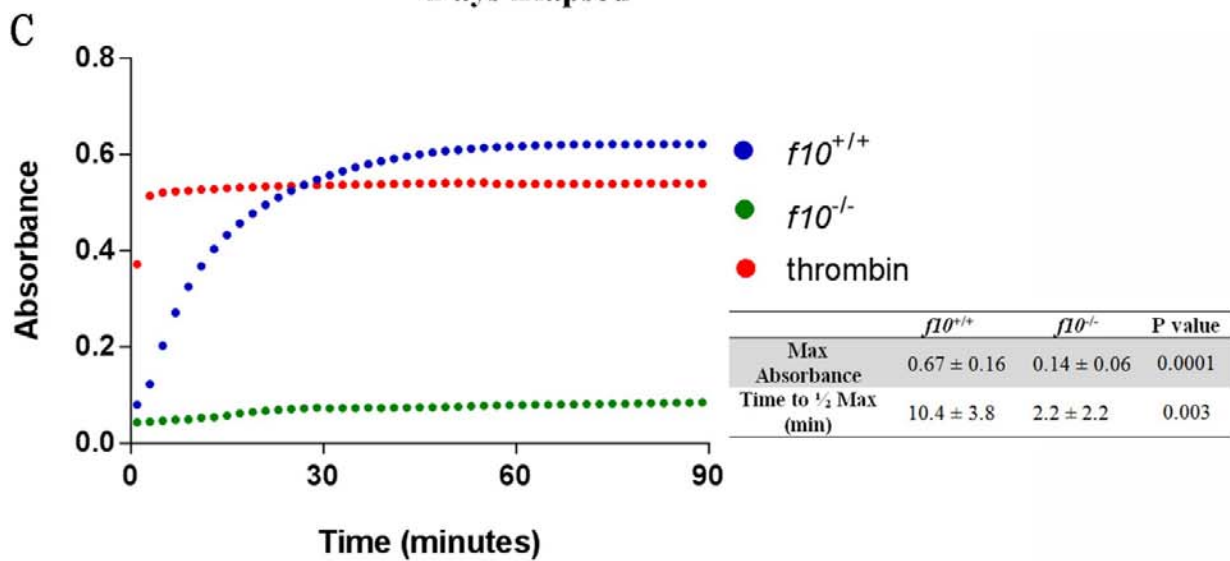
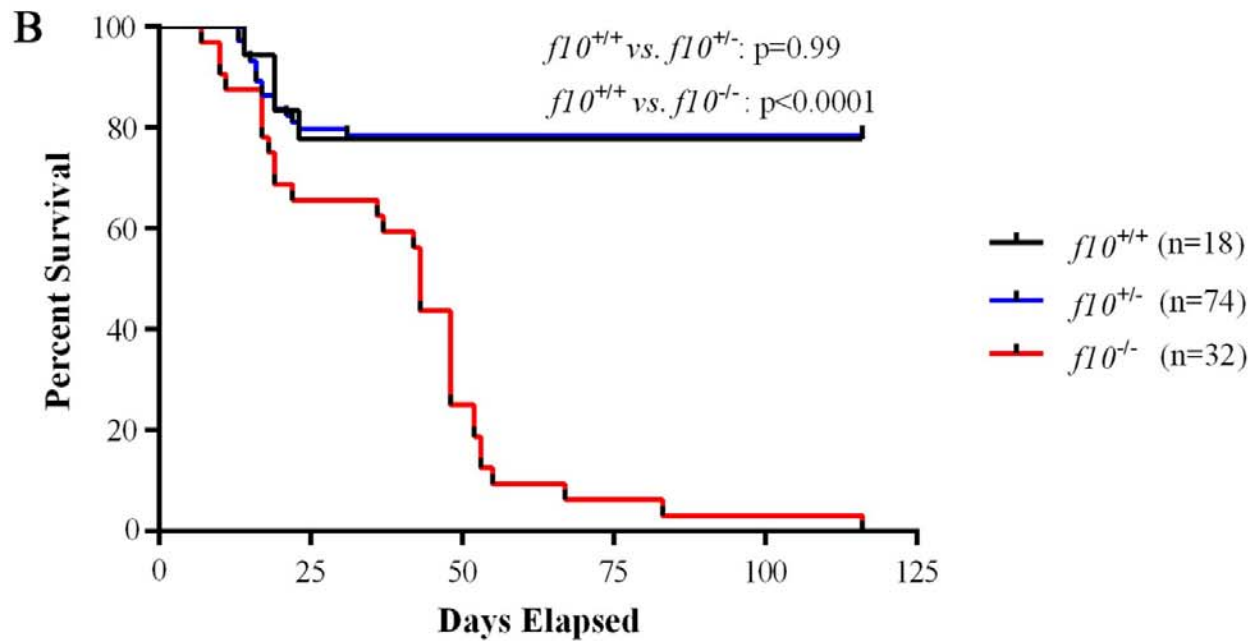


Figure 3

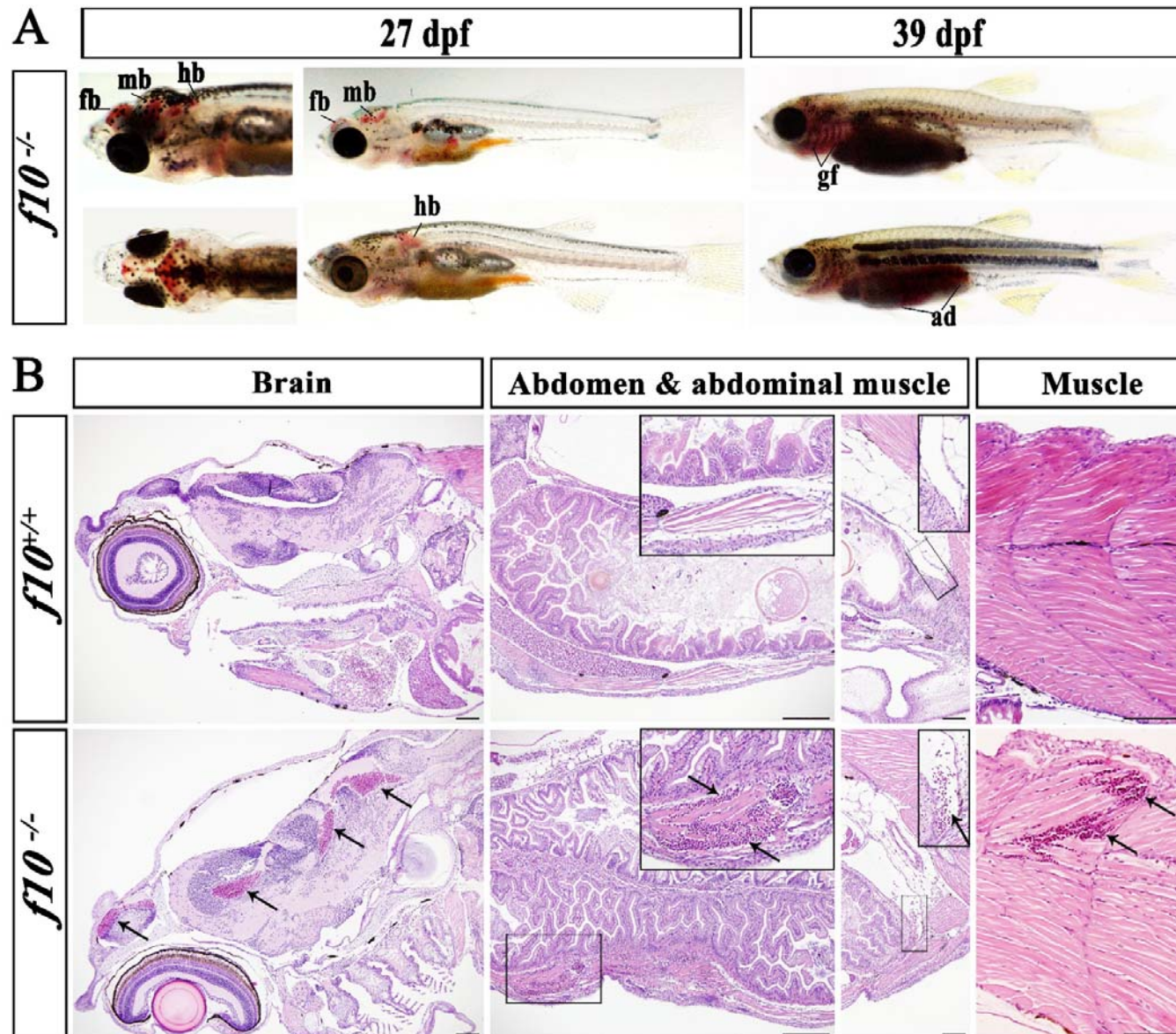


Figure 4

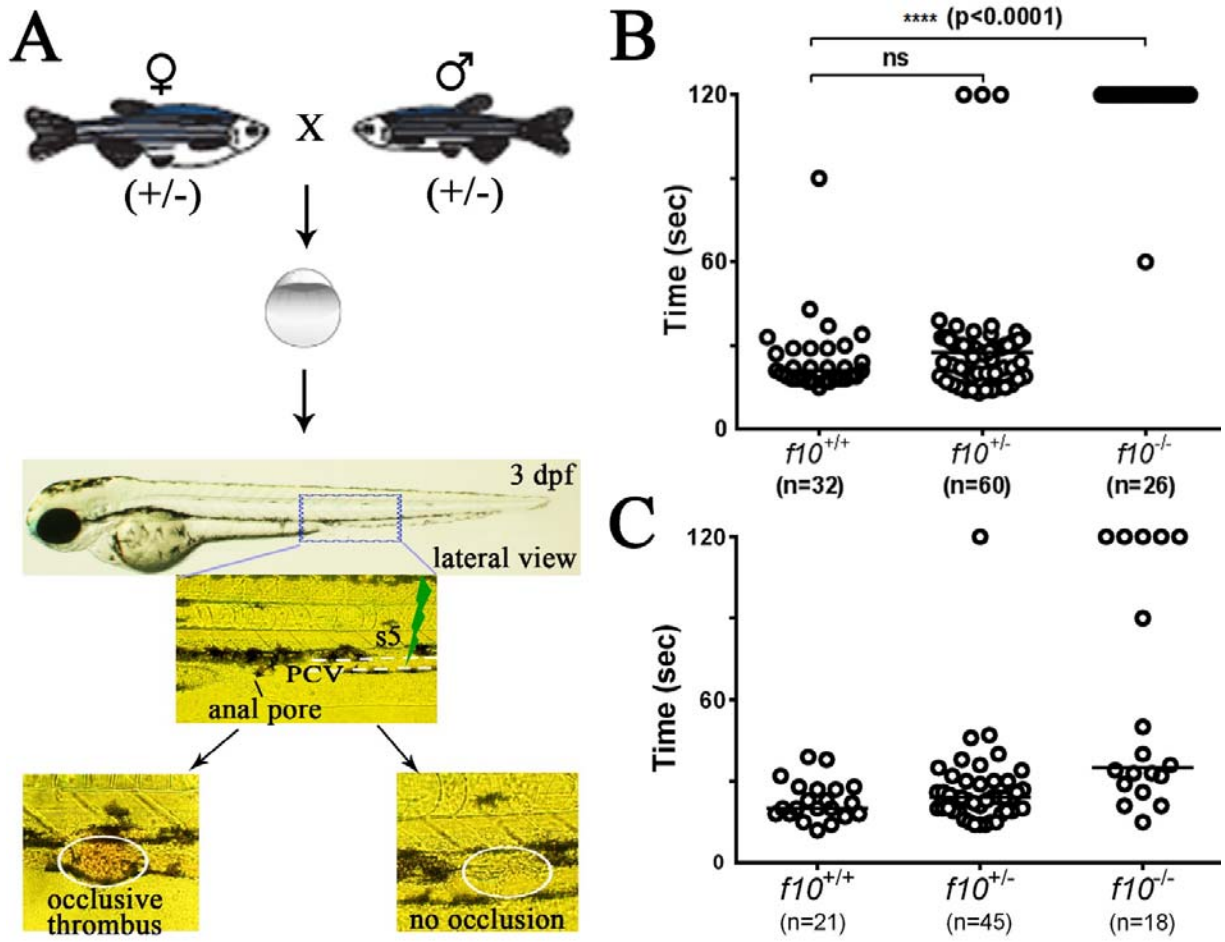


Figure 5

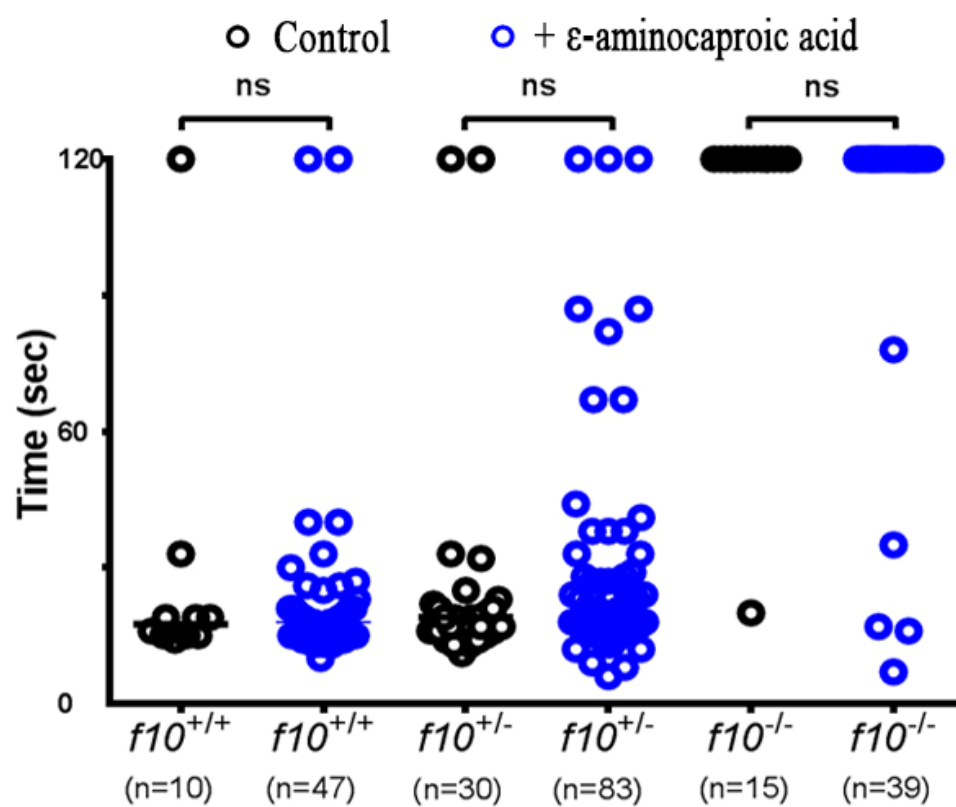


Figure 6

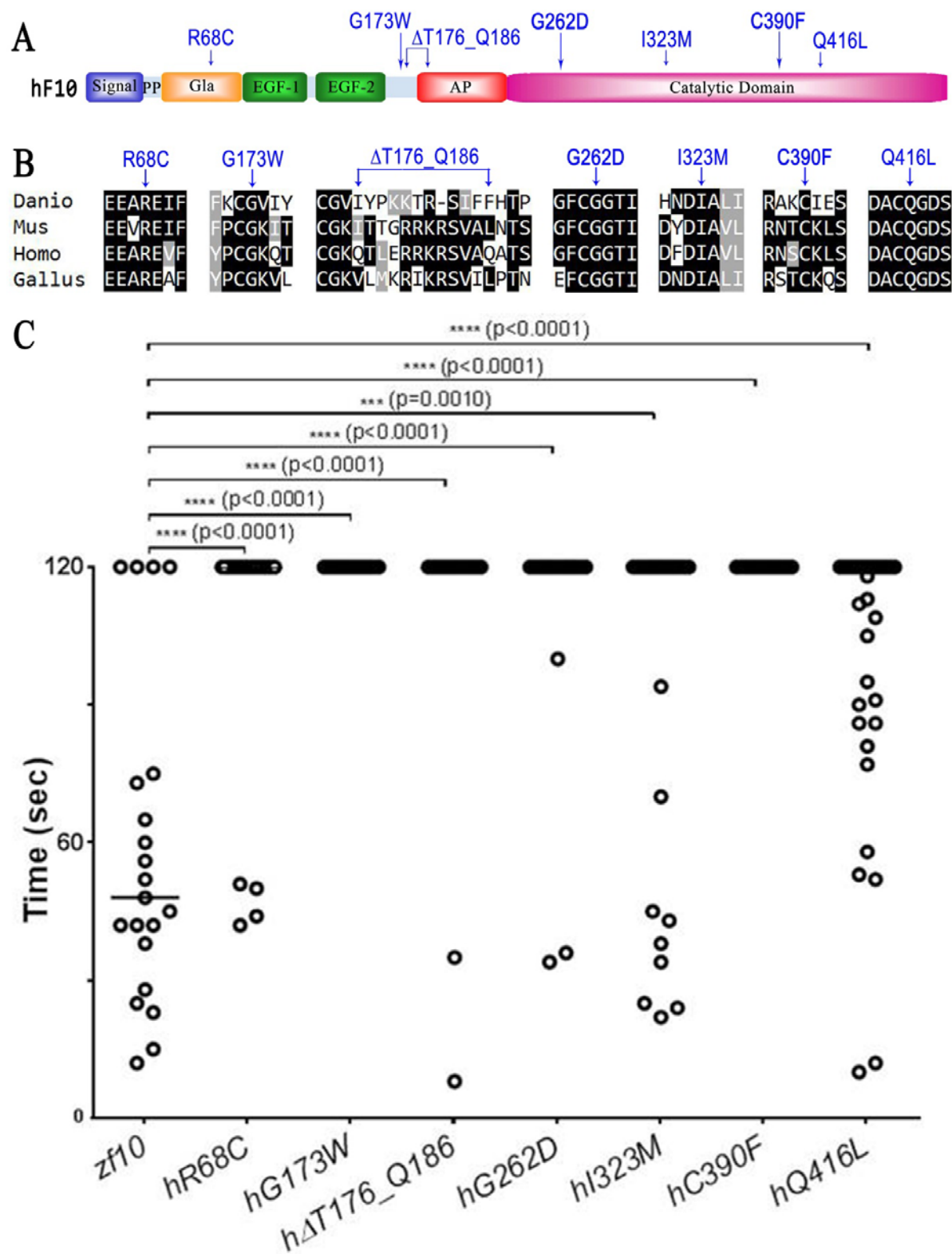


Figure 7